Available online at www.sciencedirect.com
ScienceDirect
International Journal of Heat and Mass Transfer 50 (2007) 85–93
International Journal of HEAT and MASS TRANSFER
www.elsevier.com/locate/ijhmt

Conjugate heat transfer analysis of a heat generating vertical plate

S. Jahangeer, M.K. Ramis, G. Jilani *

Department of Mechanical Engineering, National Institute of Technology, Calicut, Kerala 673 601, India

Received 26 September 2005; received in revised form 9 May 2006
Available online 29 September 2006

Abstract

This paper mainly deals with conjugate heat transfer problem pertinent to rectangular fuel element of a nuclear reactor dissipating heat into an upward moving stream of liquid sodium. Introducing boundary layer approximations, the equations governing the flow and thermal fields in the fluid domain are solved simultaneously along with two-dimensional energy equation in the solid domain by satisfying the continuity of temperature and heat flux at the solid–fluid interface. The boundary layer equations are discretized using fully implicit finite difference scheme so as to adopt marching technique solution procedure, while second-order central difference scheme is employed to discretize the energy equation in the solid domain and the resulting system of finite difference equations are solved using Line-by-Line Gauss–Seidel iterative solution procedure. Numerical results are presented for a wide range of parameters such as aspect ratio, A_r, conduction–convection parameter, N_{cc}, heat generation parameter, Q, and flow Reynolds number, Re. It is concluded that there exist an upper or a lower limiting value of these parameters above or below which the temperature in the fuel element crosses its allowable limit. It is also found that an increase in Re results in considerable increase in overall heat dissipation rate from the fuel element.

Keywords: Conjugate heat transfer; Heat generating vertical plate; Finite difference method; Rectangular fuel element

1. Introduction

The term 'conjugate heat transfer' refers to a heat transfer process involving an interaction of conduction within a solid body and the convection from the solid surface to fluid moving over the solid surface. Therefore, a realistic analysis of conjugate heat transfer problems necessitates the coupling of the conduction in the solid and the convection in the fluid. This is generally accomplished by satisfying the conditions of continuity in temperature and heat flux at the fluid–solid interface. There are many engineering devices in which conjugate heat transfer analysis becomes important. Most common example is a heat exchanger in which the conduction in the tube wall is greatly influenced by the convection in the surrounding fluid. Another example of conjugate heat transfer problem is found in fins. The conduction within the fin and convection in the fluid surrounding it must be simultaneously analyzed to obtain vital design information. The conjugate heat transfer finds yet another very important application in the fuel element of a nuclear reactor. Nuclear reactors are highly complex installations and great care needs to be exercised while designing them. The energy released due to fission in the fuel element ultimately appears in the form of heat and results in an increase in temperature of the fuel element. If this heat generated is not dissipated fast enough, the fuel elements and other components may heat up so much that eventually a part of the core may melt. In fact, the limit to the power at which a reactor can be operated is set by the heat transfer capacity of the coolant [1]. Therefore, knowledge of the temperature field, in particular the highest temperature, in the fuel element is needed in order to predict its thermal performance. The maximum allowable temperature in the fuel element is generally limited by the need to avoid undesirable changes in the material. Melting of the fuel element must be avoided, and in practice, there are

* Corresponding author. Tel.: +91 495 2286445; fax: +91 495 2287250.
E-mail address: jilani@nitc.ac.in (G. Jilani).

0017-9310/$ - see front matter © 2006 Elsevier Ltd. All rights reserved.
doi:10.1016/j.ijheatmasstransfer.2006.06.042

Nomenclature

Upper case symbols given in the parentheses are the dimensionless counterparts of the dimensional equivalents written on the same line

A_r	aspect ratio
C_p	specific heat of the coolant
k_s	thermal conductivity of fuel element material
k_f	thermal conductivity of the coolant
L	length of the fuel element
N_{cc}	conduction–convection parameter
Pr	Prandtl number
q'''	volumetric heat generation
Q	heat generation parameter
Re	Reynolds number
T	temperature
T_0	maximum allowable temperature
$u(U)$	velocity component in axial direction
$v(V)$	velocity component in transverse direction
w	half thickness of the fuel element
$x(X)$	axial co-ordinate
$y(Y)$	transverse co-ordinate

Greek symbols

θ	dimensionless temperature
α	thermal diffusivity of the coolant
ρ	density of the coolant
μ	dynamic viscosity
v	kinematic viscosity

Subscripts

∞	free stream
s	solid
f	fluid

usually other effects, which are even more restricting [2]. Due to above facts, thermal analyses of heat generating elements of rectangular as well as cylindrical geometry cooled in their surrounding medium have been the subject of many investigations in the past.

Karvinen [3] presented an approximate method for solving the conjugate heat transfer problem associated with a heat generating plate washed by forced convection flow. Sparrow and Chyu [4] studied the conjugate heat transfer problem associated with a vertical plate fin washed by laminar forced convection flow. One-dimensional conduction equation for the fin and boundary layer equations for fluid were solved simultaneously by satisfying the conditions of continuity of temperature and heat flux at the solid–fluid interface. Keeping Prandtl number fixed at 0.7 for air, the numerical results were presented for a range of values of conduction–convection parameter. Deriving motivation from this work, conjugate heat transfer problem of a plate fin washed by laminar forced convection boundary layer flow was carried out by Garg and Velusamy [5]. One-dimensional conduction equation for the fin and boundary layer equations for fluid were solved simultaneously by similarity solution approach. The results were presented for a wide range of Prandtl number and conduction–convection parameter. Yu et al. [6] proposed a very effective solution method for solving the conjugate conduction-forced convection problems. For incompressible, laminar boundary layer flow of a fluid with constant thermo-physical properties over a flat plate and a wedge, the interface temperatures and heat transfer rates were computed accurately using finite-difference scheme. Conjugate heat transfer problem associated with forced convection flow over a conducting slab sited in an aligned uniform stream was analyzed analytically as well as numerically by Vynnycky et al. [7]. For the full numerical solutions, the governing equations were first developed in dimensionless stream function–vorticity–temperature form and then solved using a finite difference scheme. The numerical results were presented for a wide range of Reynolds number, Prandtl number, aspect ratio of the slab and thermal conductivity ratio of the slab and the fluid. Recently, Jilani et al. [8] numerically studied conjugate heat transfer problem associated with a heat generating vertical cylinder washed by upward forced flow. The two-dimensional conduction equation for the heat generating cylinder and boundary layer equations for the fluid were discretized using finite difference schemes. While the two-dimensional heat conduction equation for the cylinder was solved using Line-by-Line method, marching technique solution procedure was employed to solve the boundary layer equations for the fluid. Results were presented for a wide range of aspect ratio, heat generating and conduction–convection parameters, keeping Prandtl number fixed at 0.005.

From the review of the literature presented above, it becomes abundantly clear that with the exception of Karvinen [3] and Jilani et al. [8], none of the investigators paid their attention to the conjugate heat transfer analysis of heat generating cylinder or plate. While the problem investigated by Karvinen [3] is based on one-dimensional heat conduction in the heat generating plate, the conjugate heat transfer analysis presented by Jilani et al. [8] is limited to cylindrical geometry. The prime objective of the present work is to study the conjugate heat transfer problem pertinent to rectangular nuclear fuel element dissipating fission heat into upward moving liquid sodium. Introducing boundary layer approximations, the equations governing the flow and thermal fields in the fluid domain are solved simultaneously along with two-dimensional energy equation in the solid domain by satisfying the continuity of temperature and heat flux at the solid–fluid interface. While the

boundary layer equations are discretized using fully implicit finite difference scheme so as to adopt marching technique solution procedure, a second-order central difference scheme is used to discretize the energy equation in the solid domain and the resulting system of finite difference equations are solved employing Line-by-Line Gauss–Seidel iterative solution procedure.

2. Mathematical formulation

Fig. 1 illustrates a rectangular nuclear fuel element of length L, thickness $2w$ and thermal conductivity k_s dissipating heat into streams of upward moving coolant having density ρ, dynamic viscosity μ, specific heat C_p, and thermal conductivity k_f. The free stream conditions of the coolant just at the upstream of the plate are maintained at uniform temperature T_∞ and uniform velocity u_∞. Under steady state operating conditions of the nuclear reactor, while the leading edge of the fuel element is assumed to be in perfect thermal contact with the oncoming stream of coolant, thereby, maintained at temperature T_∞, the heat loss from the trailing edge is considered to be negligibly small. The volumetric energy generation q''' due to nuclear fission reaction in the fuel element is assumed to be uniform. The total energy generated is first conducted within the fuel element and finally dissipated mainly from its lateral surface by forced convection to the upward moving streams of coolant so as to keep the maximum temperature T_0 in the fuel element well within certain permissible limit. For the mathematical formulation of the problem stated above, the following additional approximations and assumptions are introduced:

(i) The material of the fuel element is homogeneous and isotropic.
(ii) The thermal conductivity of the fuel element is independent of temperature.
(iii) The temperature gradient normal to the x–y plane is negligibly small.
(iv) The flow is steady, laminar, incompressible and two-dimensional.
(v) The coolant is Newtonian and viscous.
(vi) The thermo-physical properties of the coolant are constant.
(vii) The boundary layer approximations are valid.

In addition to geometric symmetry, the flow and thermal fields are also symmetric about the vertical axis of the fuel element, which facilitates only half of the solution domain to be taken as the computational domain. Besides, these symmetries suggest that the transverse temperature gradient along the vertical axis of the fuel element is zero. Fig. 2 depicts the computational domain indicating thereon the most appropriate boundary conditions relevant to the present study. A Cartesian co-ordinate system is superimposed on the computational domain in such a manner that bottom-left corner of the domain represents its origin.

The velocity and temperature distribution in the flow field are governed by the boundary layer equations, while the temperature distribution inside the fuel element is governed by the two-dimensional heat conduction equation. The condition at the solid–fluid interface is obtained by the requirement that the heat flux and temperature be continuous. Since the fluid velocity at the surface of the fuel element is zero due to the no slip condition, the heat transfer from the surface to the fluid in its immediate vicinity is predominantly by conduction and can, therefore, be given by Fourier's law of heat conduction.

The dimensionless form of the boundary layer equations governing the flow and thermal fields over the rectangular fuel element is given by

$$\text{Continuity}: \quad \frac{\partial U}{\partial X}+\frac{\partial V}{\partial Y_f}=0 \tag{1}$$

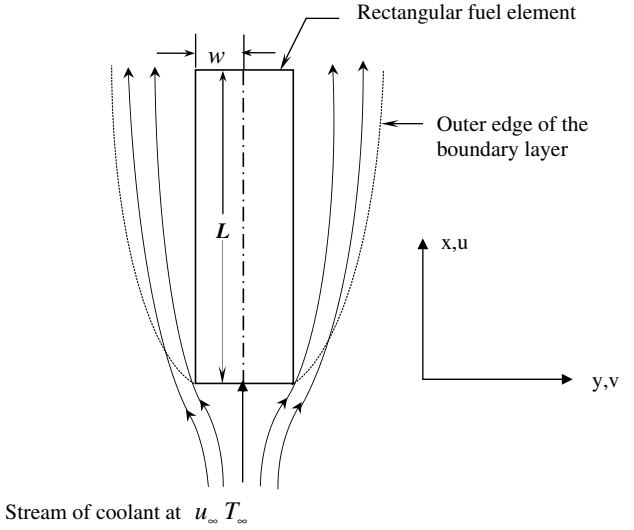

Fig. 1. Physical model.

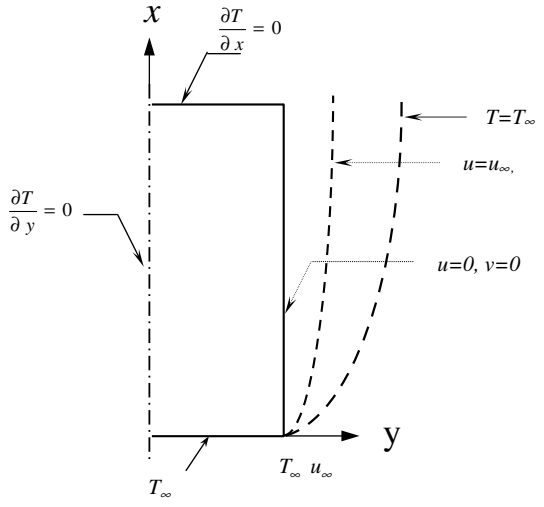

Fig. 2. Computational domain.

$$X\text{-momentum}: \quad U\frac{\partial U}{\partial X}+V\frac{\partial U}{\partial Y_f}=\frac{1}{Re}\frac{\partial^2 U}{\partial Y_f^2} \tag{2}$$

$$\text{Energy}: \quad U\frac{\partial \theta_f}{\partial X}+V\frac{\partial \theta_f}{\partial Y_f}=\frac{1}{RePr}\frac{\partial^2 \theta_f}{\partial Y_f^2} \tag{3}$$

The dimensionless form of the most appropriate boundary conditions is

$$\begin{aligned} &U(Y_f,0)=1, \quad V(Y_f,0)=0, \quad \theta_f(Y_f,0)=0\\ &U(0,X)=0, \quad V(0,X)=0\\ &U(\infty,X)=1, \quad \theta_f(\infty,X)=0 \end{aligned} \tag{4}$$

The dimensionless form of two-dimensional heat conduction equation for the plate with uniform internal heat generation is

$$\frac{\partial^2\theta}{\partial X^2}+C\frac{\partial^2\theta}{\partial Y^2}+CQ=0 \tag{5}$$

where C is a geometric parameter defined as

$$C=4A_r^2 \tag{6}$$

subject to boundary conditions:

$$\begin{aligned} &\frac{\partial\theta(0,X)}{\partial Y}=0, \quad \frac{\partial\theta(1,X)}{\partial Y}=N_{cc}\frac{\partial\theta(0,X)}{\partial Y_f}, \quad \theta(1,X)=\theta_f(0,X)\\ &\theta(Y,0)=0, \quad \frac{\partial\theta(Y,1)}{\partial X}=0 \end{aligned} \tag{7}$$

The following dimensionless parameters are used in the above equations (Eqs. (1)–(6)):

$$\begin{aligned} &X=\frac{x}{L}, \quad Y=\frac{y}{w}, \quad Y_f=\frac{y}{L}\\ &U=\frac{u}{u_\infty}, \quad V=\frac{v}{u_\infty}, \quad \theta=\frac{T-T_\infty}{T_0-T_\infty}\\ &A_r=\frac{L}{2w}, \quad Q=\frac{q'''w^2}{k_s(T_0-T_\infty)}, \quad N_{cc}=\frac{k_f}{k_s}\left[\frac{w}{L}\right]\\ &Re=\frac{u_\infty L}{v}, \quad Pr=\frac{v}{\alpha} \end{aligned} \tag{8}$$

3. Numerical solution

Eqs. (1)–(3) for the fluid and Eq. (5) for the solid are coupled and, therefore, the solution of these equations is to be obtained simultaneously by satisfying the conditions of continuity of temperature and heat flux at the solid–fluid interface. Due to obvious reasons the solution of these equations is not easily tractable by analytical means and, therefore, has to be obtained numerically. Line-by-Line Gauss–Seidel iterative method is employed for steady, two-dimensional heat conduction equation, while boundary layer equations are solved using marching technique solution procedure. While Eq. (1) is discretized so as to solve in an explicit stepwise manner, fully implicit finite difference scheme is used in the discretization of Eqs. (2) and (3). Following Hornbeck [9], Eqs. (2) and (3) are discretized using backward difference formula for the X-derivatives and central difference formulae for Y-derivatives, whereas only backward difference formula for both X- and Y-derivatives is employed to obtain finite difference form of Eq. (1). It is worth emphasizing here that the finite difference forms of Eqs. (2) and (3) possess tridiagonal structure and, therefore, are efficiently solved using famous 'Thomas Algorithm'. The step-by-step numerical solution procedure adopted for the solution of the conjugate heat transfer problem pertinent to the present work is almost similar to the one described by Jilani et al. [8] and, therefore, is not presented here for the sake of brevity.

3.1. Validation of the computer code

The numerical results presented and discussed in this paper are obtained using a computer code developed exclusively for the present work. The validity of the entire code is established in two ways. At first, the validity of the part of the code dealing with solid domain is ascertained by comparing the analytically obtained transverse temperature distribution at an axial location, $X=0.50$ corresponding to a slightly modified computational domain with that computed using the present code. It is worth emphasizing here that three out of four boundary conditions are exactly the same for both modified and actual models and that volumetric heat generation source of the present problem is replaced by constant temperature heat source at the solid–fluid interface so as to make the modified model physically well posed. Table 1 demonstrates such a comparison. It is abundantly clear from the results presented in this table that analytically obtained temperature values are in excellent agreement with those computed using the code. The validity of the remaining part of the code dealing with the fluid domain is examined by comparing the computed flow field with Blasius solution. Figs. 3(a) and 3(b) demonstrates such a comparison. While Fig. 3(a) illustrates the comparison of the distribution of stream-wise component of velocity, U at the axial location $X=0.1$, a similar comparison for the axial location $X=1.0$ is demonstrated in Fig. 3(b). It is very much clear from these two figures that numerically obtained U-component of velocity profiles are in excellent agreement with those obtained from Blasius solution. At this point it must be made clear that above part-wise validation of the code do authenticate the complete code as whole since the algorithm for computing

Table 1
Transverse temperature distribution in the modified computational domain at $X=0.5$

Y	Analytical	Numerical
0.20	0.38	0.38
0.40	0.45	0.45
0.60	0.57	0.57
0.80	0.75	0.75
1.00	1.00	1.00

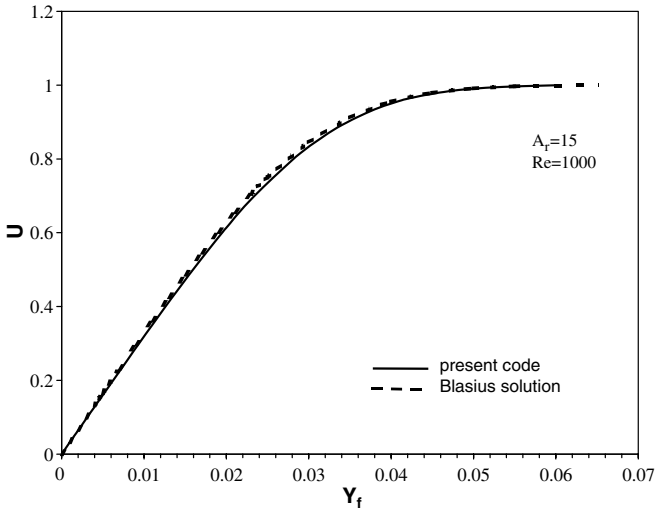

Fig. 3(a). Comparison of numerically computed U-velocity profile with that obtained from Blasius solution at an axial location $X = 0.1$.

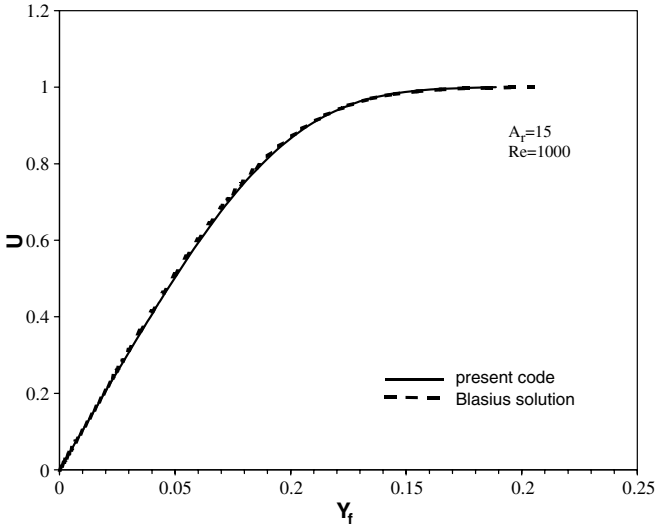

Fig. 3(b). Comparison of numerically computed U-velocity profile with that obtained from Blasius solution at an axial location $X = 1.0$.

the temperature field in the fluid domain is almost similar to that of obtaining velocity field. However, in the absence of experimental or numerical data similar to this study, the present code in its entirety is also validated by means of energy balance. Table 2 demonstrates the comparison of the total energy generated within the fuel element as input to the code with the sum of energy being dissipated from heat transfer surface, which, in turn, is obtained from the computed temperature fields using the present code as output. It is evident from this table that the sum of 'heat generation parameter equivalent' corresponding to bottom surface, Q_{bs} and lateral surfaces, Q_{ls} obtained as output from the computer code is in excellent agreement with the heat generation parameter, Q which is given as input to the code.

Table 2
Validation of the computer code for conjugate heat transfer problem using energy balance for fixed $A_r = 15$, $N_{cc} = 0.4$, and $Re = 1000$

Heat generation parameter, Q (as input)	'Heat generation parameter equivalent' at the two heat dissipating surfaces		
	Bottom surface, Q_{bs} (1)	Lateral surface, Q_{ls} (2)	Sum of (1) and (2)
0.25	0.0058	0.2444	0.2502
0.50	0.0117	0.4881	0.4998
0.75	0.0175	0.7323	0.7498
1.00	0.0234	0.9765	0.9999
1.25	0.0292	1.2206	1.2498

3.2. Grid independence test

A series of numerical experiments are conducted to arrive at optimum grid sizes to be used for generating numerical data pertinent to present work. As expected, it

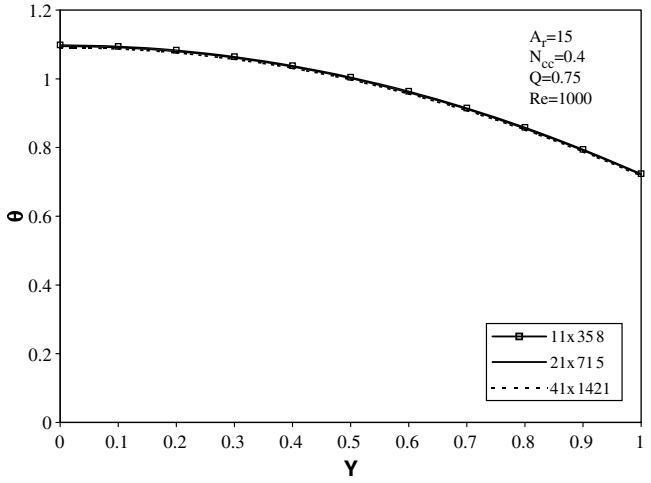

Fig. 4(a). Transverse temperature profiles at $X = 0.5$ in the fuel element for three different grid sizes.

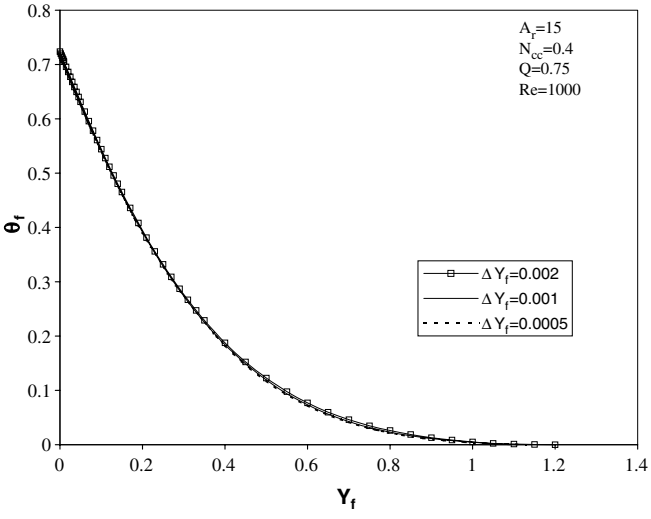

Fig. 4(b). Transverse temperature profiles at $X = 0.5$ in the coolant for three different grid sizes.

is observed that computational grid strongly depends on flow Reynolds number, Re. Therefore, different optimum grid sizes depending on the value of Re has been used in the computation associated with the present study. Figs. 4(a) and 4(b) demonstrates the typical grid independence test performed for $Re = 1000$ while keeping $A_r = 15$, $N_{cc} = 0.4$, and $Q = 0.75$ fixed. It can be seen that transverse temperature profiles in the fuel element as well as in the fluid domain corresponding to three different grid sizes, i.e. (11 × 358), (21 × 715), and (41 × 1421) almost overlap each other. Further, taking into consideration of better resolution of zero-Neumann boundary conditions and energy balance, optimum grid sizes of (21 × 715) is employed in the case of $Re = 1000$.

4. Results and discussion

The prime objective of the present investigation is to obtain the critical parameters, which govern the safe and optimum operating conditions of nuclear reactors. Accordingly, keeping the value of Prandtl number, Pr for liquid sodium as coolant to be constant at 0.005, numerical results in the form of transverse temperature profiles, critical parameters, axial temperature profiles, and average Nusselt number are presented and discussed in detail for a wide range of aspect ratio A_r, heat generation parameter Q, conduction–convection parameter N_{cc}, and Reynolds number Re.

The effect of A_r on transverse temperature profiles at the axial location, $X = 0.5$ in the fuel element, keeping $N_{cc} = 0.4$, $Q = 0.75$, and $Re = 2500$ fixed, is depicted in Fig. 5. It can be easily noted from this figure that initially, an increase in A_r results in an appreciable increase in the temperature of the fuel element and in the surface heat dissipation rate. However, this effect diminishes sharply with further increase in A_r and finally leads to a transverse temperature profile, which is independent of A_r. Thus, it can be concluded that there exists an optimum value of A_r for which heat dissipation rate from the plate is maximum.

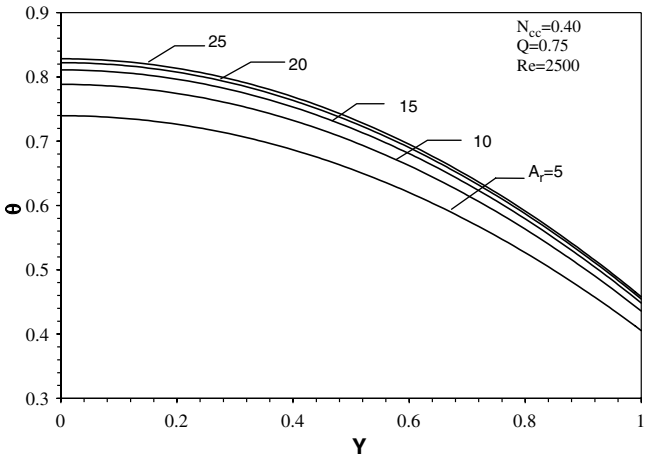

Fig. 5. The effect of A_r on transverse temperature profiles at the axial location $X = 0.5$ and for fixed values of $N_{cc} = 0.4$, $Q = 0.75$, and $Re = 2500$.

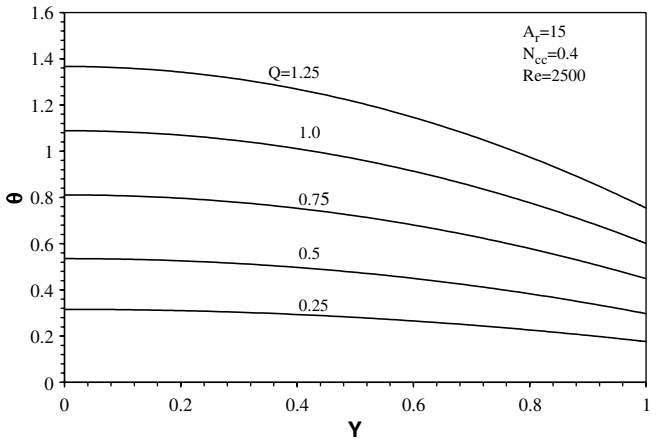

Fig. 6(a). The effect of Q on transverse temperature profiles at the axial location $X = 0.5$ and for fixed values of $A_r = 15$, $N_{cc} = 0.4$, and $Re = 2500$.

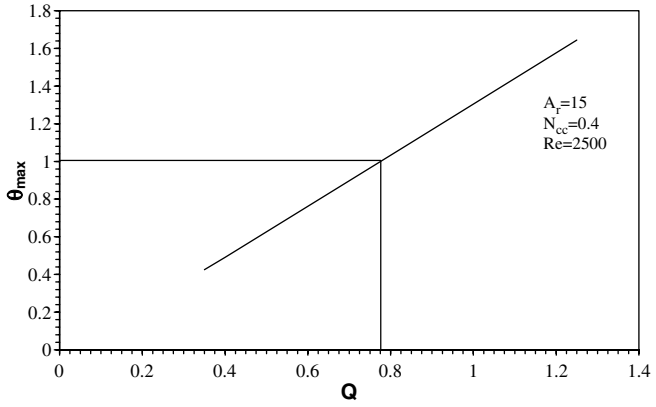

Fig. 6(b). The variation of θ_{max} with Q for fixed values of $A_r = 15$, $N_{cc} = 0.4$, and $Re = 2500$.

Fig. 6(a) shows the effect of Q on transverse temperature distribution in the rectangular fuel element of a nuclear reactor at the axial location $X = 0.5$, keeping A_r, N_{cc}, and Re fixed at 15, 0.4, and 2500, respectively. It is worth noticing that the temperature of the fuel element in general and temperature gradient at its lateral surface in particular increases sharply with increase in Q. The above trend may be due to the fact that all the energy generated within the element, N_{cc} and Re being kept fixed, cannot be dissipated to the surrounding coolant resulting in energy storage and higher surface heat dissipation rate. Although, the maximum temperature in the fuel element is not explicitly indicated in this figure, it can be easily inferred that there exists a limiting value of Q beyond which maximum temperature in the fuel element, θ_{max} exceeds its allowable limit. The variation of θ_{max} with Q, while $A_r = 15$, $N_{cc} = 0.4$, and $Re = 2500$ being kept fixed, is depicted in Fig. 6(b). For this set of constant parameters, upper limiting value of heat generation parameter, i.e., $Q_l = 0.775$,

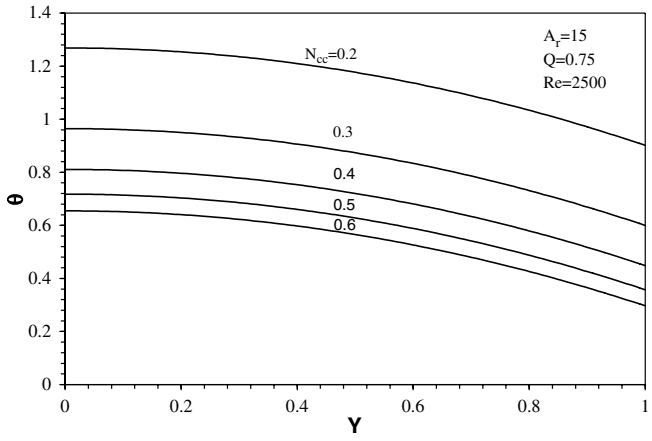

Fig. 7(a). The effect of N_{cc} on transverse temperature profiles at the axial location $X = 0.5$ and for fixed values of $A_r = 15$, $Q = 0.75$, and $Re = 2500$.

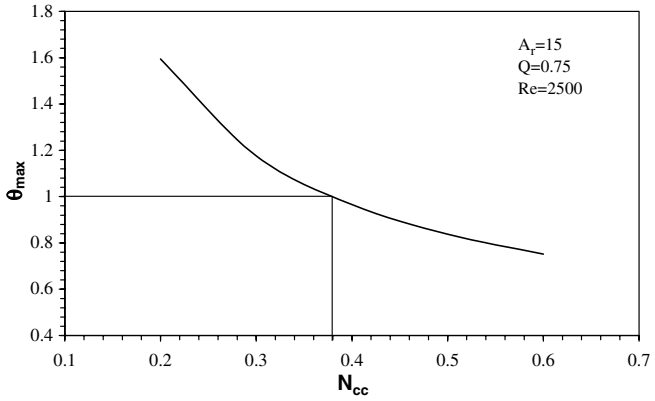

Fig. 7(b). The variation of θ_{max} with N_{cc} for fixed values of $A_r = 15$, $Q = 0.75$, and $Re = 2500$.

which corresponds to $\theta_{max} = 1$, can be easily noted from this figure.

The effect of N_{cc} on the transverse temperature distribution in the fuel element at the axial location $X = 0.5$, while $A_r = 15$, $Q = 0.75$, and $Re = 2500$ being kept fixed, is illustrated in Fig. 7(a). It is abundantly clear from this figure that as N_{cc} increases initially from 0.2 to 0.3, temperature of the fuel element decreases considerably. However, further increase in N_{cc} results in relatively small decrease in fuel element temperature and finally this decrease in fuel element temperature due to increase in N_{cc} becomes almost insignificant for all values of $N_{cc} \geqslant 0.5$. The above trend may be attributed to the higher rate of energy dissipation from the fuel element to the coolant due to increase in N_{cc} from its lower value. On the other hand, as Q being kept fixed, further increase in N_{cc} results in only marginal increase in energy dissipation rate because there is a natural limit beyond which energy dissipation rate can not be further increased. Like Fig. 6(a), this figure too does not explicitly specify θ_{max} value in the fuel element. Fig. 7(b) shows the variation of θ_{max} with N_{cc} for a set of fixed value of $A_r = 15$, $Q = 0.75$, and $Re = 2500$. The lower limiting

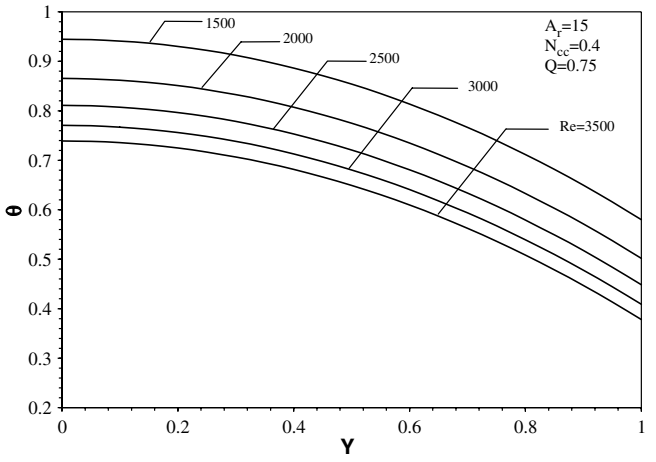

Fig. 8(a). The effect of Re on transverse temperature profiles at the axial location $X = 0.5$ and for fixed values of $A_r = 15$, $N_{cc} = 0.4$, and $Q = 0.75$.

value of N_{cc} equal to 0.38, which corresponds to $\theta_{max} = 1$, can be easily noted from this figure.

Fig. 8(a) depicts the effect of Re on the transverse temperature profiles at the axial location $X = 0.5$ in the fuel element for fixed values of $A_r = 15$, $N_{cc} = 0.4$, and $Q = 0.75$. As expected, it is quite clear from this figure that increase in Re results in decrease in temperature in the fuel element. This may be attributed to higher surface heat dissipation rate due to increase in convection effect associated with increase in Re values. It is also worth noticing that decrease in temperature in the fuel element due to increase in Re is comparatively more pronounced for lower range of values of Re than its higher range of values. It is important to emphasize here that although the transverse temperature profiles in this figure does not indicate the maximum temperature in the fuel element, it is quite likely that maximum temperature in the fuel element may exceed its allowable limit. For the same fixed set of values of parameters, i.e., $A_r = 15$, $N_{cc} = 0.4$, and $Q = 0.75$, Fig. 8(b) clearly indicates that there exists a lower limiting value of Re below which it cannot be further decreased, otherwise the temperature

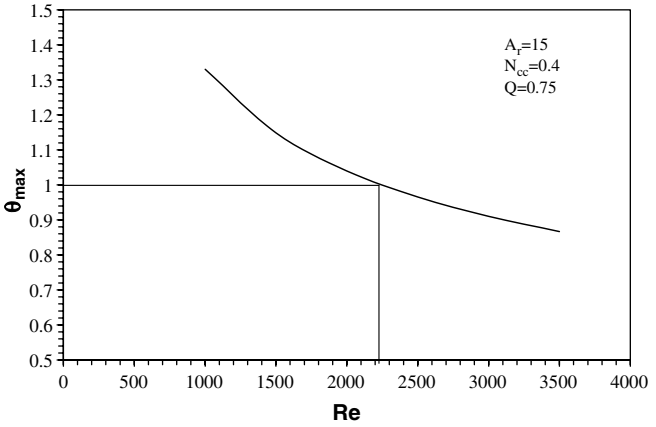

Fig. 8(b). The variation of θ_{max} with Re for fixed values of $A_r = 15$, $N_{cc} = 0.4$, and $Q = 0.75$.

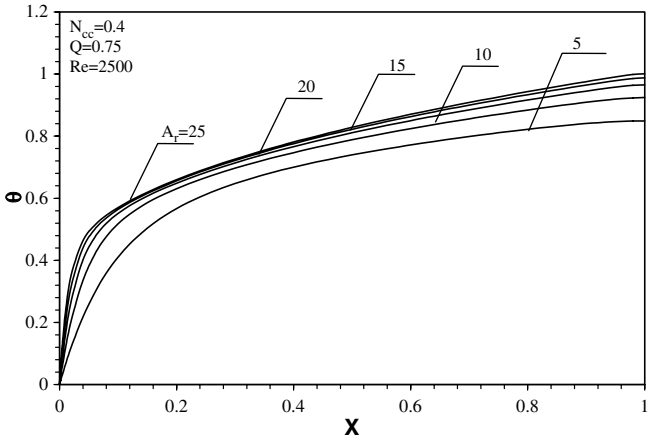

Fig. 9. The effect of A_r on axial temperature profiles along the vertical axis of the fuel element for fixed values of $N_{cc} = 0.4$, $Q = 0.75$, and $Re = 2500$.

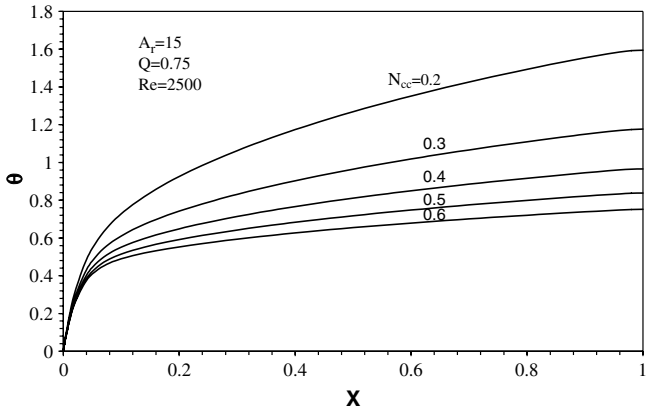

Fig. 11. The effect of N_{cc} on axial temperature profiles along the vertical axis of the fuel element for fixed values of $A_r = 15$, $Q = 0.75$, and $Re = 2500$.

anywhere in the fuel element will certainly cross its permissible limit.

Fig. 9 illustrates the effect of A_r on the axial temperature profiles in the fuel element, while the values of $N_{cc} = 0.4$, $Q = 0.75$, and $Re = 2500$ being kept fixed. As expected, it is very well apparent from this figure that temperature in the fuel element along its axial direction increases sharply up to certain distance from the leading edge and thereafter increase in temperature becomes more or less smooth. It is quite interesting to observe that as A_r increases, the difference in two consecutive axial temperature profiles diminishes rapidly and finally becomes invariant for all $A_r \geqslant 20$.

Fig. 10 shows the effect of Q on axial temperature profiles obtained for the set of fixed values of $A_r = 15$, $N_{cc} = 0.4$, and $Re = 2500$. As noticed earlier in Fig. 9, it can be noted from this figure as well that for any value of Q, axial temperature gradient in the fuel element is much steeper at axial locations near the leading edge as compared to the one away from it. As expected, these sharp axial temperature gradients near the leading edge become more and more pronounced with increase in Q. Interestingly, unlike Fig. 9, the axial temperature gradients away from the leading edge of the fuel element show strong dependency on the value of Q. It can be easily noted that axial temperature profiles for lower values of Q is more or less flat in contrast to the same for higher values of Q. From the thermal design point of view, it is important to emphasize here that there exists an upper limiting value of Q above which it cannot be further increased, otherwise it may lead to disastrous effects due to obvious reasons.

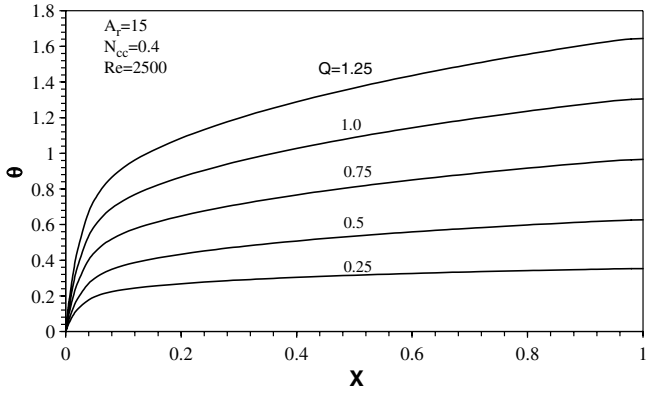

Fig. 10. The effect of Q on axial temperature profiles along the vertical axis of the fuel element for fixed values of $A_r = 15$, $N_{cc} = 0.4$, and $Re = 2500$.

The effect of N_{cc} on the axial temperature profiles in the fuel element for the set of values of $A_r = 15$, $Q = 0.75$, and $Re = 2500$ is illustrated in Fig. 11. It can be easily noticed that irrespective of the value of N_{cc}, axial temperature profiles corresponding to all locations $X \leqslant 0.04$ more or less overlap each other in contrast to those shown in Figs. 9 and 10. However, these axial temperature profiles near the leading edge too tend to become more and more pronounced with decrease in the value of N_{cc}. It is also important to note that a decrease in N_{cc} results in a relatively steeper axial temperature profiles at locations away from the leading edge, which may be attributed to reduction in surface heat dissipation rate due to decrease in N_{cc}. Further, it can be noted that the rate of increase in axial temperature increases with decrease in N_{cc}. Interestingly enough, it is quite important to observe that there is a lower limiting value of N_{cc} below which the maximum temperature in the fuel element exceeds its allowable limit.

Fig. 12 shows the effect of Re on the axial temperature distribution along the vertical axis of the fuel element for constant values of $A_r = 15$, $Q = 0.75$, and $N_{cc} = 0.4$. Interestingly enough, as noticed in Fig. 11 for different values of N_{cc}, the axial temperature profiles corresponding to all axial locations $X \leqslant 0.06$ more or less overlap each other irrespective of the value of Re. While the axial temperature profiles near the leading edge still have sharp gradients, axial temperature profiles gradually become more and more smooth as one move away from the leading edge of the fuel element. As expected, increase in Re results in still more and more flat axial temperature profiles away from the leading edge. It is interesting to note that initial increase

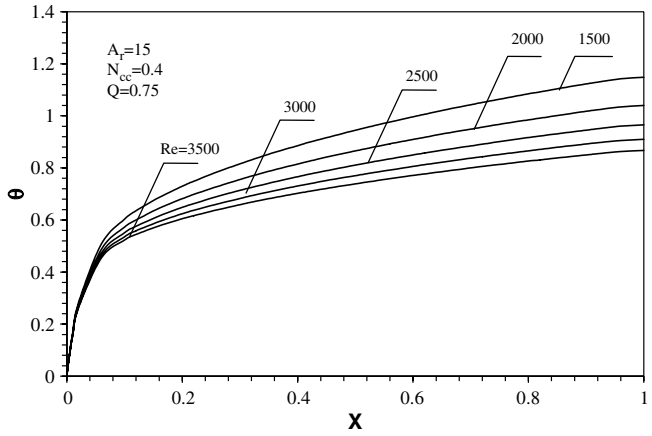

Fig. 12. The effect of Re on axial temperature profiles along the vertical axis of the fuel element for fixed values of $A_r = 15$, $N_{cc} = 0.4$, and $Q = 0.75$.

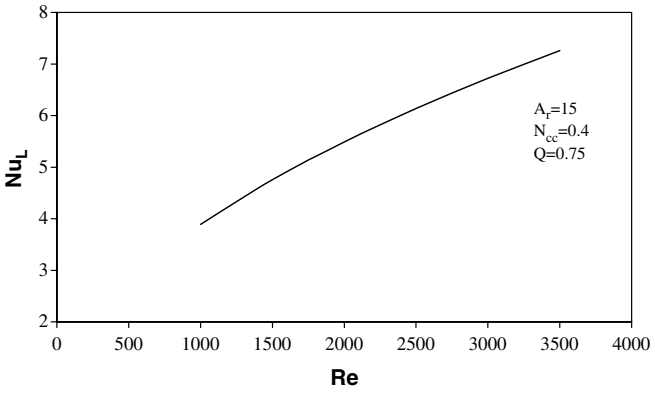

Fig. 13. The effect of Re on average Nusselt number, Nu_L for fixed values of $A_r = 15$, $N_{cc} = 0.4$, and $Q = 0.75$.

in Re from 1500 to 2000 results in an appreciable decrease in the axial temperature of the fuel element. However, as Re is increased further, the rate of decrease in axial temperature with respect to increase in Re gradually decreases and ultimately attain a profile which is independent of Re. From thermal design point of view of a nuclear reactor, it can be further concluded that there is a lower limiting value of Re below which it cannot be decreased in order to maintain the temperature anywhere within the fuel element under permissible limit.

Fig. 13 depicts variation of average Nusselt number, Nu_L with Re, while $A_r = 15$, $N_{cc} = 0.4$, and $Q = 0.75$ being kept fixed. It can be easily inferred from this figure that as expected, an increase in Re results in considerable increase in Nu_L, i.e., increase in heat transfer from the fuel element to the surrounding coolant. This is due to the fact that increase in Re indirectly implies increase in mass flow rate of the coolant, which in turn results in increased heat dissipation rate from the lateral surface of the fuel element. Above trend is quite desirable from the point of view of safe operation of nuclear reactors with reasonably high power capacity. Interestingly enough, it is observed that Nu_L remains invariant with any of the parameters – A_r, N_{cc}, and Q, while the rest of other relevant parameters being kept fixed.

5. Conclusions

This paper deals with the conjugate heat transfer analysis of a rectangular fuel element of a nuclear reactor dissipating fission heat into upward moving liquid sodium as coolant. Accordingly, two-dimensional heat conduction equation for the fuel element and two-dimensional boundary layer equations for the coolant are solved simultaneously by satisfying the continuity of temperature and heat flux at the solid–fluid interface. Numerical results in the form of transverse temperature profiles, axial temperature profiles, and average Nusselt number are presented for a wide range of parameters such as aspect ratio, A_r, conduction–convection parameter, N_{cc}, heat generation parameter, Q, and flow Reynolds number, Re. It is concluded that there exist a lower limiting value of N_{cc} and Re below which the temperature within the fuel element crosses its allowable limit. It is also observed that there exists an upper limiting value of Q above which the temperature within the fuel element crosses its allowable limit. Interestingly enough, it is found that while the average Nusselt number, Nu_L remains more or less invariant with any of the parameters – A_r, N_{cc}, and Q, increase in Re results in significant increase in Nu_L.

References

[1] S. Garg, F. Ahmed, L.S. Kothari, Physics of Nuclear Reactor, Tata McGraw-Hill, New Delhi, 1986.
[2] R.H.S. Winterton, Thermal Design of Nuclear Reactors, Pergamon Press, Oxford, 1981.
[3] R. Karvinen, Some new results for conjugated heat transfer in a flat plate, Int. J. Heat Mass Transfer 21 (1978) 1261–1264.
[4] E.M. Sparrow, M.K. Chyu, Conjugate forced convection-conduction analysis of heat transfer in plate fin, Int. J. Heat Mass Transfer 104 (1982) 204–206.
[5] V.K. Garg, K. Velusamy, Heat transfer characteristics for a plate fin, ASME J. Heat Transfer 108 (1986) 224–226.
[6] W.-S. Yu, H.-T. Lin, T.-Y. Hwang, Conjugate heat transfer of conduction and forced convection along wedges and a rotating cone, Int. J. Heat Mass Transfer 34 (1991) 2497–2507.
[7] M. Vynnycky, S. Kimura, K. Kanev, I. Pop, Forced convection heat transfer from a flat plate: the conjugate problem, Int. J. Heat Mass Transfer 41 (1998) 45–59.
[8] G. Jilani, S. Jayaraj, M.A. Ahmed, Conjugate forced convection conduction heat transfer analysis of a heat generating vertical cylinder, Int. J. Heat Mass Transfer 45 (2002) 331–341.
[9] R.W. Hornbeck, Numerical Marching Techniques in Fluid Flows with Heat Transfer, NASA, Washington, DC, 1973.